 doi:10.20944/preprints202104.0271.v1

Article

Impact of Sodium Hexametaphosphate on the flotation of ultrafine magnesite from dolomite-rich desliming tailings

Duong Huu Hoang[1,2], Doreen Ebert[1], Robert Möckel[1] and Martin Rudolph[1]

[1] Helmholtz Institute Freiberg for Resource Technology, Helmholtz-Zentrum Dresden-Rossendorf, Chemnitzer Straße 40, 09599 Freiberg, Germany

[2] Maelgwyn Mineral Services Ltd, Ty Maelgwyn, 1A Gower Road, Cathays, Cardiff, CF24 4PA, United Kingdom

* Correspondence: d.hoang@hzdr.de or dhoang@maelgwyn.com

Abstract: Depletion of ore deposits, increasing demand for raw materials, the need to process low-grade, complex and finely disseminated ores and the reprocessing of tailings are challenges especially for froth flotation separation technologies. Even though capable of handling relatively fine grain sizes the flotation separation of very fine and ultrafine particles faces many problems still. Further, the flotation of low-contrast semi-soluble salt-type minerals with very similar surface properties, many complex interactions between minerals, reagents and dissolved species often result in poor selectivity. This study investigates the flotation beneficiation of ultrafine magnesite rich in dolomite from desliming, currently reported to the tailings. The paper especially focuses on the impact of the depressant sodium hexametaphosphate (SHMP) on: (i) the froth properties using dynamic froth analysis (DFA), (ii) the separation between magnesite and dolomite/calcite and (iii) its effect on the entrainment. Furthermore, the application of 1-hydroxyethylene-1,1-diphosphonic acid (HEDP) as a more environmentally friendly and low-cost alternative to SHMP is presented and discussed. The paper contributes to understanding on the complexity of depressant responses in froth flotation.

Keywords: magnesite, dolomite, semi-soluble salt-type minerals, tailings, sodium hexametaphosphate SHMP, 1-hydroxyethylene-1,1-diphosphonic acid HEDP, Dynamic Froth Analyzer, froth properties, remining, pneumatic Imhoflot, reactor-separator, FineFuture

1. Introduction

Continuously decreasing ore grades and the ever-increasing demand for raw materials by more sustainable means requires exploration and processing of low-grade and complex ores, with fine-grained composition, the reprocessing of tailings and beneficiation of fine-grained particles in the processing plants. However, it's broadly known that the flotation separation of fines and ultrafine particles faces many challenges, like less effective particle-bubble collisions and reduced attachment probabilities (affecting negatively the recovery), increasing unselective entrainment and activation of gangue and thus true flotation of gangue (affecting negatively the concentrate grade).

The flotation separation of magnesium-bearing carbonates (magnesite and dolomite) from non-salt type minerals (hematite, gold-bearing sulfides, and monazite) is typically less difficult as compared to their separation from other salt-type minerals [1]. However, flotation of semi-soluble salt-type minerals which contain a significant amount of $(CO_3)^{-2}$ along with Mg^{2+}/ Ca^{2+} ions [2-4] is generally challenging. These dissolved ions and in consequence their solution species will also interact with various minerals changing their surface properties, which interfere with the added reagents, affecting collector-mineral interactions, consuming reagents and influencing flotation performance [1]. For instance, Ca^{2+} ion can interact with $(CO_3)^{-2}$ to form $CaCO_3$ and precipitate on the magnesite surface and change the magnesite's surface properties, which can then be falsely depressed. Such interferences are the main reason for poor reagent selectivity, i.e., separation contrast [5]. The solution thermodynamics of systems containing various suspended semi-soluble salt-type minerals and flotation reagents are rather complex. In addition to the dissolution of minerals and adsorption of dissolved mineral and reagent species at the interface, interactions between these species in the bulk can lead to complicated phenomena such as surface and bulk precipitation as well as re-dissolution of adsorbed species [5]. Due to surface reactions, the lattice is disrupted and a new phase can be formed, so that surface precipitation may occur in the interfacial or subsurface region [6]. Competition of the dissolved mineral species with similarly

 doi:10.20944/preprints202104.0271.v1

charged collector species for adsorption sites can result in the depression of mineral flotation. The reagents interact not only with the exposed surface of magnesite but also with dolomite and calcite which then exhibit weak hydrophobic surface properties, leading to true flotation of these gangue minerals.

Theoretically, the flotation separation of carbonate minerals can be achieved by direct flotation of magnesite with depression of calcium-bearing carbonates (dolomite and calcite) and silicate gangue minerals; reverse flotation of calcium carbonates and/or silica with depression of the magnesite and a combination of reverse (amine flotation) of silicates and direct magnesite flotation. However, in most cases, both magnesite and calcium-bearing carbonates show similar responses to the reagents. All minerals, i.e., magnesite ($MgCO_3$), dolomite ($CaMg(CO_3)_2$) and calcite ($CaCO_3$) belong to the group of semi-soluble salt-type minerals with similar cations (Ca^{2+}/ Mg^{2+}) [3].

Conventional collectors such as fatty and rosin acids have been a fairly standard family of collectors for the separation of calcium/magnesium minerals and their mechanism of adsorption has been widely studied [7]. However, there is a tendency to absorb onto slime, i.e., fine particle surfaces, and high temperature is often a requirement with relatively high reagent consumption. Application of fatty acids as the collectors along with the depression of gangue minerals is the conventional way to selectively separate calcium/ magnesium minerals. However, this has a low selectivity, limited success and increasing processing costs, hence it is not always satisfactory on an industrial level [8]. Therefore, different types of collectors are considered in the flotation of calcium-bearing minerals [8,9], including oleates, hydroxamates, sulfosuccinates and sarcosinate. The mixtures of collectors have been showing more favorable improvements on selectivity than using only one collector [10] [11,12] [8,13]. However, in the absence of depressants or modifiers, collectors respond to both magnesite and calcium carbonate gangues (dolomite and calcite) are similar, their recoveries are in roughly equal proportion and the overall flotation is not selectively efficient [1,14,15]. The depressants play a critical role in improving the selectivity, especially for the flotation separation of semi-soluble salt-type minerals.

Furthermore, it is widely known that the main uses of depressant regulators in flotation are their great capability for dispersion, modification of froth properties, control of pH, precipitation and/or complexation of metallic ions, and modification of collector action [1,16]. In semi-soluble salt flotation systems, the main depressants are including inorganic and organic [17,18], e.g. sodium carbonate, sodium silicate, sodium pyrophosphate [19], sodium hexametaphosphate (SHMP), starch, carboxymethyl cellulose (CMC), quebracho and tannin derivatives [20]. However, due to the similarity in surface properties of magnesite and calcium-bearing carbonates, the depressants not only depress gangue minerals but can also depress the valuable mineral. The fine particles have interactive effects on each other that could depress another mineral [21], fine particles of magnesium carbonates can coat the surface of their associated mineral and depress them [22-24]. SHMP can also interact with free calcium/ magnesium ions in the pulp and prevent the formation of unwanted salt minerals. The interaction between the depressants, free ions, other reagents and mineral surfaces in the semi-soluble salt-type minerals is very complex.

Yin, *et al.* [25] indicated that a chelation inhibitor 1, 2-bis (o-aminophenoxy) ethane-N,N,N′,N′-tetra acetic acid (BAPTA) can improve the separation efficiency of magnesite and dolomite. However, its high production costs and the studies were conducted on single minerals, limiting the utilization to industrial practice [14]. Sodium hexametaphosphate (SHMP, $(NaPO_3)_6$) is often used in water treatment as water softener, which preventing the formation of unwanted salts such as limescale and interference with some cations (Ca^{2+}, Mg^{2+}, $Fe^{2+/3+}$, etc.). In mineral flotation, it is used as a depressant, which is well-known that it has an excellent capability of dispersion, complexation of metal ions and modifications of reagents action [1]. However, it had a wastewater problem and as a dispersant, thus negatively affecting the liquid-solid separation, such as filtration and thickening processes.

Despite only a few studies addressing the impact of sodium hexametaphosphate on the sulphide ore flotation in seawater [26-29], very little attention has been paid to the semi-soluble salt-type minerals, in particular for magnesite ore containing carbonate gangue minerals (dolomite, calcite).

Luo, Wei, Shen, Han and Zhang [15] stated that using sodium carbonate as a regulator/ co-depressant [30] together with SHMP gave better recovery compared to using SHMP alone. Also, the reagents addition order is essential when the SHMP is added prior to Na_2CO_3, eliminating the adverse effect of Ca^{2+}. SHMP interacts with Ca^{2+} or Mg^{2+} ions, preventing the formation of $CaCO_3$, or $MgCO_3$ on the mineral surfaces, which reduced the

hydrophobicity of the magnesite surface. However, we have conducted some tests using different addition orders but obtained the negative results, there was increased consumption of collector to achieve the same recovery.

1-hydroxyethylene-1,1-diphosphonic acid (HEDP) has been used as an environmental water treatment reagent due to its low cost and excellent anti-scaling performance in an aqueous solution to prevent the precipitation of calcium salts, i.e., in low-pressure boilers, oil field operations and cool water systems [31]. Recently, the application of HEDP serving as a flotation reagent showed a promising result. Huang, *et al.* [32] found out that HEDP has been used as a selective flotation reagent of chalcopyrite against pyrite. HEDP has also been proven to be a good fluorite inhibitor in separating fluorite from calcite via reverse flotation [33]. Furthermore, a recent study by Yang, Wang, Cao, Yin, Xue, Zhu, Fu and Yao [14] using HEDP as a depressant in single phase minerals displayed very selective depression of dolomite due to the HEDP strongly adsorbing onto dolomite with a higher calcium site density [14], whereas it had only slightly shown to depress magnesite.

This present study investigates the effect of SHMP on the flotation separation of ultrafine magnesite rich in dolomite from desliming tailings in the lab batch scale. Its impact on the pulp and froth properties using additional sedimentation tests and a dynamic froth analyser (DFA), support the investigation to understand how SHMP application links the flotation performance, entrainment and downstream processes. Furthermore, the paper also presents the application of HEDP as a selective depressant, which could be considered for SHMP's replacement.

2. Materials and Methods

2.1. Materials

Magnesitas Navarras (Magna) was founded in 1945. Magna is one of the world's leading companies as a vertically integrated producer of magnesium oxide (MgO) based solutions and materials for the steelmaking, agriculture, livestock and environmental sectors. The beneficiation of the mineral has different process and one of them is the flotation of low-grade magnesite. At this stage, the ore is ground to below 0.2 mm for the sake of liberation. The mill discharge is passed through a hydrocyclone to separate the slimes (-25 μm) to the tailings ponds, with a mass pull of approx. 20 % (w/w). Flotation is only conducted on the underflow with the particle size of about 25 μm - 200 μm and involves two-stages flotation, i.e., amine flotation to remove silicates and direct flotation of magnesite.

The material used in this study is the cyclone overflow (d_{80} = 17 μm), so-called slime tailings. It is currently discharging to the tailings ponds due to no suitable separation method to treat this fine material. The fine reject contains about (52.3 -60) % (w/w) magnesite, (33 - 36.9) % dolomite, (3 - 3.5) % calcite, (3.4 - 4.4) % quartz and 3.4 % other minerals (see section 3.2).

2.2. Reagents

Sodium carbonate (Na_2CO_3, 99.9 %) as a pH regulator was used to achieve an alkaline environment, it also acts as a co-depressant/ multi-faceted reagent [30]. Sodium silicate (Na_2SiO_3) as a dispersant agent, also depressant, with a purity of 99 %, was supplied by Zschimmer & Schwarz GmbH & Co. KG, Germany. Sodium hexametaphosphate (SHMP-$Na_6O_{18}P_6$) was supplied by Alfa Aesar. 1-Hydroxyethane-1,1-diphosphonic acid (HEDP) used as depressant, with a purity of 90 % was from Carl Roth GmbH. Methyl isobutyl carbinol (MIBC) was utilized as a frother provided by Sigma-Aldrich, Germany. The Resanol A100 was used as a magnesite collector provided by Ekof GmbH, Germany. Short reagent conditioning time and staged addition are applied to prevent the slime generation and reagent consumption [1], i.e., SHMP, HEDP and Resanol A100 were added in at different steps, the first addition to receive concentrates 1 and 2. Then the air supply is stoped. The additional reagents are added and conditioned before air is turned back on and concentrates 3 to 5 are collected. The detailed reagents regime used are given in

 doi:10.20944/preprints202104.0271.v1

Table 1.

 doi:10.20944/preprints202104.0271.v1

Table 1. Reagents regime used in flotation tests

Type	Name	Purpose	Dosage	Conditioning time (min)
pH regulator	Sodium carbonate (Na_2CO_3)	pH adjustment (co-depressant)	(to reach pH 10)	5
Depressant	Sodium silicate (Na_2SiO_3)	depresses silicates mainly	300 g/t	2
	Sodium hexametaphosphate $Na_6O_{18}P_6$	depresses calcium-bearing carbonate gangue mainly	(100 – 600) g/t (additional 2x 50 g/t added before C3, C4 and C5	2
	1-Hydroxyethane-1,1-diphosphonic acid (HEDP) $C_2H_8O_7P_2$	depresses calcium-bearing carbonate gangue mainly	200 g/t + 3x50 g/t	2
Collector	Resanol A100	magnesite collector	300 g/t, then 3x 300 g/t added before C3, C4 and C5.	3
Frother	Methyl isobutyl carbinol (MIBC)	Frother	30 g/t	2

2.3. Froth flotation experiments

The flotation tests were carried out using a 2 dm^3 Outotec GTK laboratory mechanical cell. The reagents were conditioned at a high solid concentration at 60 % (w/w), i.e., 150 g of fine magnesite ore and 100 ml of tap water. After conditioning with the reagents, the slurry is transferred into the 2 dm^3 cell. Another 1700 ml of tap water is added to achieve a solid content of 7.7 % (w/w). The pulp density is chosen relatively low due to the ultrafine size of the feed.

The impeller speed and airflow rate were adjusted at 1200 min^{-1} and 2 l/min (normal condition). The pulp's pH after adding fine magnesite lies at about 8.8, using Na_2CO_3 it is adjusted to pH10. Also, the pulp level is kept constant by adding tap water into the flotation cell when required.

For the cleaning stages, in order to have a similar pulp density, the rougher flotation was conducted twice. The concentrates from two roughers were then transferred to the first cleaner stage. The concentrate of the first cleaner then feeds the second cleaning and so on. Four cleaning stages have been conducted. There were no additional reagents prior to the cleaning stages.

After carrying out the flotation tests, all the concentrates, middlings and final tailings were filtered, dried and weighed. For the mineralogical characterization, the concentrates and tailings were analysed with XRD and Rietveld analysis at the Helmholtz Institute Freiberg for Resource Technology (HZDR/HIF), Freiberg, Germany.

2.4. Sedimentation test

The suspensions used in sedimentation tests received the same conditioning as used in the flotation test, including high solid concentration conditioning and then dilution with tap water. Only 75 g of fine magnesite samples were conditioned with 50 g tap water in a 400 ml beaker with reagents added at speed 600 rpm. The reagent regime was similar to the batch flotation (cf. section 2.3), the sodium hexametaphosphate dosage was varied, i.e. 0 g/t, 100 g/t, 200 g/t, 300 g/t, 400 g/t and 700 g/t. After conditioning, the pulp was transferred into a 500 ml graduated cylinder with a diameter of 54 mm. The cylinders were stoppered and shaken manually for

1 min, the cylinders were then left to stand, and the height of sediment is read by time. The sedimentation ratio was calculated as the ratio of the height of the clear water H_t at the time t to the initial (total) height H_0 of suspension. Also, the settling speed ($v_{settling,t}$) was defined as the different height $\Delta H(t)$ between initial height H_0 and the height of the clear water H_t at the time t divided to the settling time t.

2.5. Dynamic froth analysis

Up to now, to the best of our knowledge there is no investigation on how depressants such as SHMP effect the froth properties by means of froth stability. While conducting the flotation tests, it is observed that the froth appearance was changed with the change of depressant dosages. To evaluate the effect of SHMP on the froth ability and froth stability (i.e. froth height with time and bubble size distributions) and better understand how this links to the flotation results the dynamic froth analysis (DFA) is used. In the DFA technique, the froth rises within a column and the height is measured as a function of time. A more detailed description of the measurement procedures can be found in Hoang, *et al.* [34].

Several indicators have been introduced for the assessment of the froth stability, including froth half-life time, froth maximum height at equilibrium, bubble growth across the froth phase, air recovery and solid loading on bubbles on the top of the froth surface, froth velocity, and froth rising velocity [35]. The maximum height can be well correlated with the frothing ability and froth stability [36,37]. Bikerman [38] introduced the dynamic stability factor ($\sum$) as the ratio of the maximum volume of generated foam or froth to the gas flowrate given by Eq. 1. This factor has been used in froth flotation studies, e.g. by Mackay, *et al.* [39], McFadzean, *et al.* [40] and McFadzean, *et al.* [41].

$$\sum = \frac{V_f}{Q} = \frac{H_{\max} A}{Q} \qquad \text{Eq. 1}$$

where V_f is the froth volume, Q is the gas flowrate, H_{max} is the maximum equilibrium height and A is the cross-sectional area of the column.

The half-life time of the bubbles can be used to evaluate froth stability as well. In this study, it is determined as the times between the reached maximum froth height and stable froth.

The pulp suspensions used for the dynamic froth analysis are prepared such as the ones used in the batch flotation and sedimentation tests. The fresh suspensions have been prepared for each test to prevent aging effects of the pulp properties. Each condition had been measured in triplicates. A 60 ml sample of this pulp is transferred to a transparent glass column of 40 mm inner diameter of the DFA-100 (Krüss, Germany). The froth is generated by bubbling air through a ceramic frit (pore diameter 16 µm – 45 µm) at 0.4 l/min air flow rate for a constant duration of 100 s. The froth properties, including its height and structure, are recorded to evaluate dynamic parameters of the frothing ability, froth stability and time-dependent bubble size distributions. The bubble size distribution is observed at a fixed camera position (60 mm), froth height and employing an adapted image processing algorithm described in section 3.3.2 below.

2.6. Mineral Liberation Analysis and quantitative phase detection

Representative feed sample were prepared as A-side grain mounts as described in [42] and carbon coated. MLA is a FEI Quanta 650F scanning electron microscope equipped with two Bruker Quantax X-Flash 5030 EDX detectors and FEI's MLA Suite 3.1.4 for automated data acquisition [43]. MLA measurements were conducted at the Helmholtz Institute Freiberg using the GMAP method and at an accelerating voltage of 25 kV and a beam current of 10 nA. The details of MLA measurements can be found elsewhere [44,45]. The feed, concentrates and tailings were analysed using X-Ray diffraction (XRD) and quantitative compositional information is retrieved with the Rietveld method. A PANalytical Empyrean X-ray Diffractometer with a Co-tube (with primary Fe-filter) was used and operated at 35 kV and 35 mA, PIXcel 3D medipix 1x1 area detector. The measurement range was 5-80° 2 theta with a step size of 0.013° 2 theta, and the measurement time was 2.5 hours. The PDF-4+ 2020 database (ICDD) and Highscore Software package of PDF-4+ PANalytical as well as the BGMN/Profex software package [46] was used for the data evaluation.

 doi:10.20944/preprints202104.0271.v1

3. Results and Discussions

3.1. Particle and grain sizes

Figure 1 displays the particle and mineral grain size distributions as derived from MLA data with the representative particle/ grain size being the equivalent equal circle diameter (ECD). The slime magnesite tailings sample comprises slightly coarser dolomite and finer grained quartz and other minerals. It can be seen in **Figure 1** the mean particle size and d_{80} are approximately 14 µm and 17 µm, respectively. Ultrafine particles cause the challenge in conventional froth flotation. Also, ultrafine hydrophilic quartz is another issue affecting the entrainment in the case of direct flotation of magnesite.

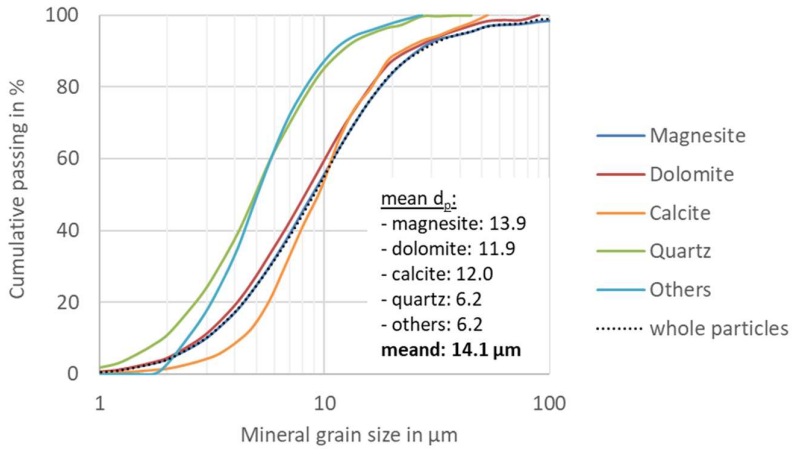

Figure 1. Cummulative particle and mineral grain size distributions derived from MLA with the size being the equivalent circle diameters (ECD) of the particle/grain sections

3.2. Mineral composition and liberation

Figure 2 and **Table 2** illustrate the mineral composition of fine magnesite ore which was analysed by automated mineralogy - MLA and XRD. MLA measurement shows that the magnesite grade is lower than the grade determined by XRD, while the dolomite content is higher as analysed with MLA (**Table 2**). It is in general an analytical challenge to distinguish between ultrafine magnesite and other magnesium-carbonates phases due to mineralogical property similarities between two minerals. Also, the discrepancy of the two methods might be caused by the minimum detectable ultrafine grain size for MLA, i.e., below 5 µm. In addition, XRD measurements indicate that there was no significant differential effect of regrinding due to the fine particles (**Table 2**). Therefore, all the concentrate and tailings samples were handled with XRD without further grinding. Furthermore, the back-calculated mineral composition from the concentrates and tailings are similar to the feed. It demonstrates that the sample preparation and chemical analysis are representative and accurate.

The ore contains about (52.3 – 60) % (w/w) magnesite, (33 - 36.9) % dolomite, (3 - 3.5) % calcite, (3.4 - 4.4) % quartz and 3.4 % other minerals (mainly clinochlore and muscovite). The main problematic gangue minerals are dolomite and calcite. All valuable magnesite ($MgCO_3$), unwanted dolomite ($MgCa(CO_3)$) and calcite ($CaCO_3$) gangue minerals belong to the group of semi-soluble salt-type minerals with calcium/magnesium-bearing exhibiting similar surface properties to magnesite (solubility, surface species, zeta potential) as well as similar responses to reagents.

Preprints (www.preprints.org) | NOT PEER-REVIEWED | Posted: 9 April 2021 doi:10.20944/preprints202104.0271.v1

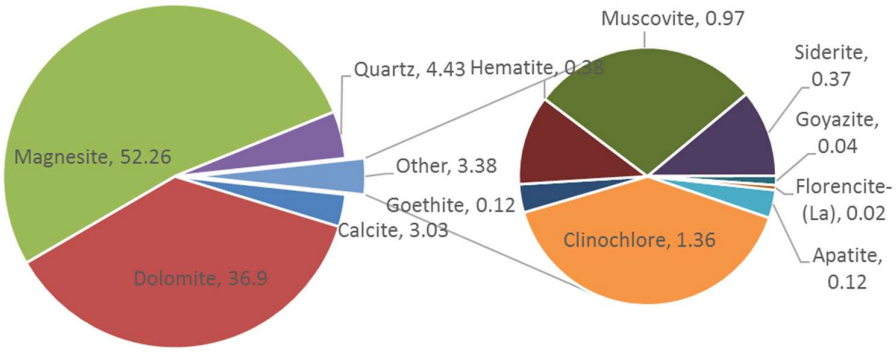

Figure 2. Mineral composition (values as % (w/w)) as analysed by MLA

Table 2. Comparison between MLA and XRD measurements

Mineral	MLA, % (w/w)	XRD, % (w/w)		
		with fine milling	without milling	back-calculated (products from flotation tests)
magnesite	52.2	58.9	60.3	59.8
dolomite	36.9	33.9	33.2	33.0
calcite	3.0	3.1	3.2	3.5
quartz	4.4	4.1	3.4	3.7
others	3.4	-	-	-
total	**100.0**	**100.0**	**100.0**	**100.0**

The mineral association results from MLA are given in Figure 3. The main gangue interlocked with magnesite consists mostly of dolomite and a bit of calcite. On the other hand, it shows that dolomite is associated mainly with magnesite.

Figure 3 displays that the main gangues interlocked with magnesite consists of dolomite 66.5 %. In contrast, magnesite is the main mineral associated with dolomite (52.9 %).

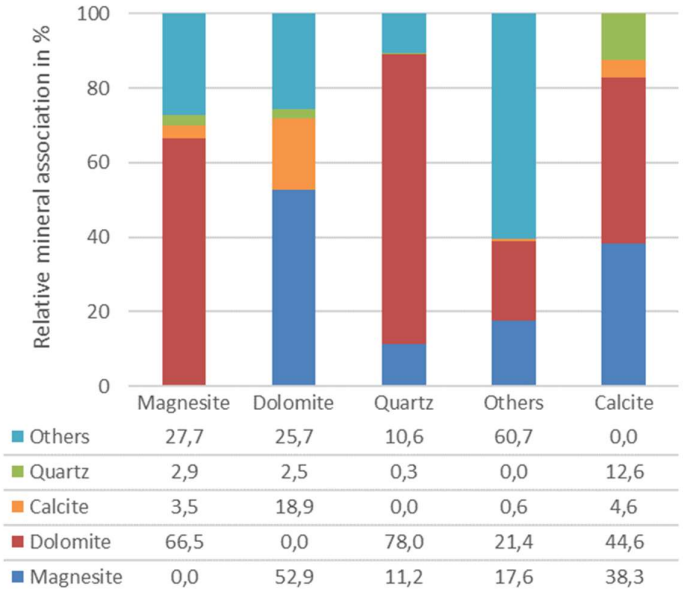

Figure 3. Mineral association (as analysed with MLA)

Preprints (www.preprints.org) | NOT PEER-REVIEWED | Posted: 9 April 2021 doi:10.20944/preprints202104.0271.v1

The theoretical grade-recovery is given in **Figure 4**. It can be seen that both valuable magnesite and gangue minerals are well liberated. However, there is a lower liberation for the calcite.

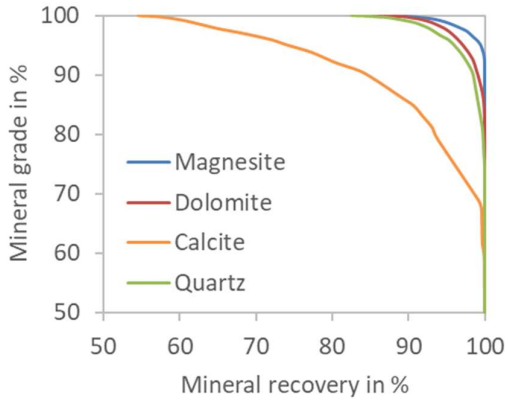

Figure 4. Mineralogical limiting curves (as analysed with MLA)

3.3. Froth properties

3.3.1. Frothing ability and froth stability

As mentioned above, SHMP is often used in water treatment as water softener, which prevents scaling by precipitation of calcium and magnesium salts. In the three-phase system with the presence of the semi-soluble salt-type minerals, many complex interactions between ions, reagents and mineral surfaces occur within the bulk solution. Hence, SHMP is expected to have a significant effect on the pulp and froth properties in general. **Figure 5** shows that as the SHMP concentration increases, the froth height decreases, decreasing the frothing ability, resulting in lower recovery (see section 0). We assume that the SHMP interacts with free Mg^{2+}, Ca^{2+} ions in the bulk. In Hoang, *et al.* [47] we argued that the attached fine particles on the bubble surfaces can prevent the bubble coalescence, reducing the bubble burst rate, thus increasing both frothing ability as well as froth stability. The higher solid content within the froth phase for the lower SHMP concentration (see **Figure 13**) could in addition be an influence on the frothing ability. After the froth reached maximum height, it reduced quickly while the gas flow rate was constant still and before bubbling was stopped at 100 s, which corresponds to the froth stability, i.e., bubble burst rate (**Figure 5**).

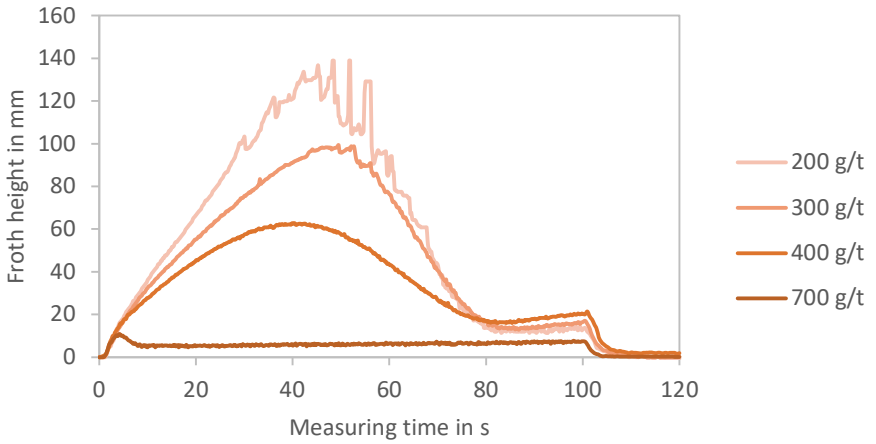

Figure 5. Froth height as a function of measuring time during growth of froth of pulp samples at different SHMP concentration as determined with the DFA method

Preprints (www.preprints.org) | NOT PEER-REVIEWED | Posted: 9 April 2021 doi:10.20944/preprints202104.0271.v1

The dynamic stability factor ∑ calculated using Eq. 1, where h_{max} is determined from Figure 5, A = 1256.6 mm² and Q = 0.4 l/min. **Figure 6** displays both the half-life time of bubble ($t_{1/2}$) and the dynamic stability factor ∑ decreasing with an increased SHMP dosage. The dynamic stability factor ∑ reduced from 0.47 to 0.03 with increasing the SHMP dosage from 200 g/t to 700 g/t, respectively. The decreasing of the dynamic stability factor and half-life time of the bubbles with an increasing the SHMP concentration causes the reduction of the recovery (see **Figure 11**) and the entrainment of the fine gangue particles (**Figure 14**).

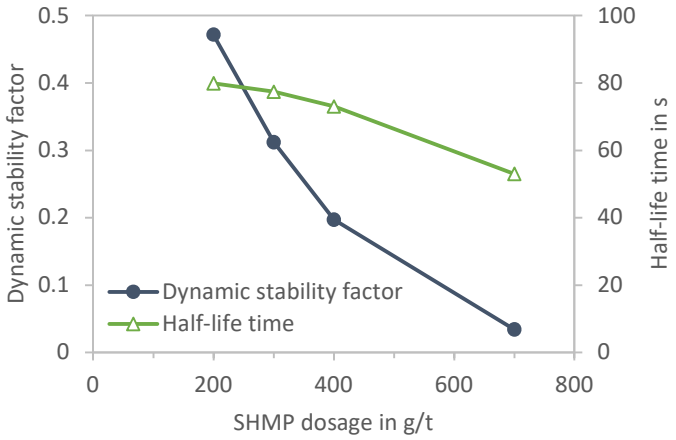

Figure 6. Half-life time of bubble $t_{1/2}$ and dynamic stability factor ∑ as a function of SHMP concentration as determined with the DFA method

3.3.2. Image processing and bubble size evaluation

The image processing is treated similarly to the method proposed by Boos, *et al.* [48], which we described in Hoang, Heitkam, Kupka, Hassanzadeh, Peuker and Rudolph [34]. Firstly, gaussian filtering with a radius of 20 pixels is employed in order to smoothen distortions from the particles positioned inside the lamellas (**Figure 7**b). Subsequently, binarization (**Figure 7**c) and a skeleton transformation (**Figure 7**d) virtually removes the thick, wall-touching Plateau borders and reveals the contact lines of the lamellas at the wall separating the bubbles. Each area bound by a set of contact lines represents the contact area of one bubble with the wall. Segmentation (**Figure 7**d) yields the size of all contact areas in the field of view. Objects close to the rim of the image or with an area smaller than 10 px² are ignored. The blue circles in **Figure 7**d mark all accepted bubble contact areas.

The bubble size is represented by the equivalent spherical radius r of the bubble volume and the contact area size is denoted by its equivalent circular radius r_s. Using the Surface Evolver, Wang and Neethling [49] found the statistics for the relation of r and r_s:

$$f\left(\frac{r_s}{r}\right) = \frac{3.51(r_s/r)^{4.61}}{1 + exp\left(47.96(r_s/r - 1.08)\right)} \quad \text{Eq. 2}$$

The bubble size distribution of all the bubbles from all images presented in **Figure 8**, as shown, the bubble sizes are increased with increasing the SHMP concentration. These findings are in line with the changes in froth height, reduction of solid content in the froth phase and reagents concentration, thus higher chances for the bubble coalescence while increasing the bubble burst rate as increasing SHMP dosage. This is certainly assuming that the semi-equilibrium bubble size within the pulp is not affected by the SHMP concentration, which is an assumption to be checked in future studies.

Preprints (www.preprints.org) | NOT PEER-REVIEWED | Posted: 9 April 2021 doi:10.20944/preprints202104.0271.v1

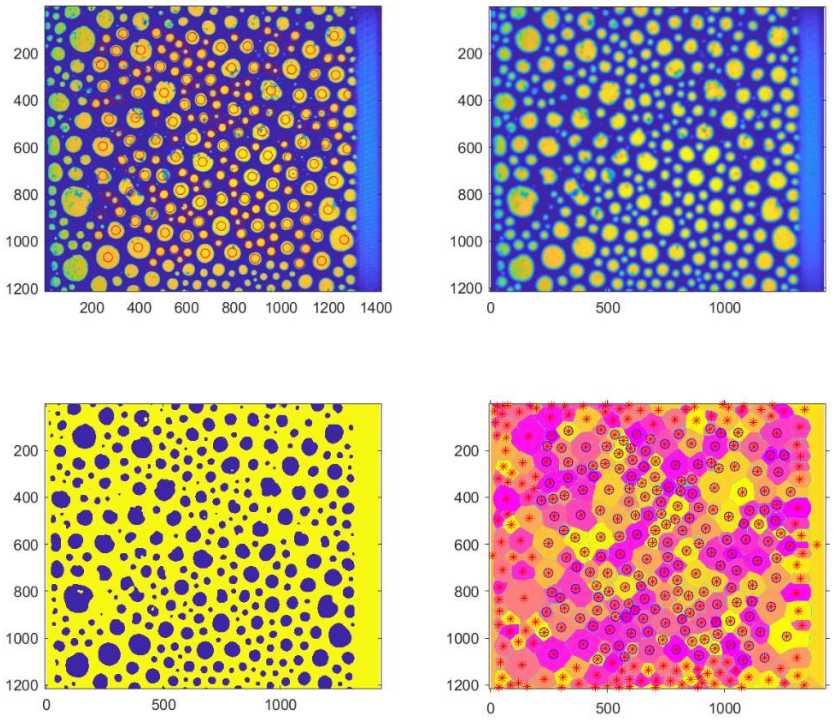

Figure 7. Bubble size evaluation with original frame obtained from DFA 100 a) filtered image b) binarized image c) and the cell skeleton image d) analysed bubbles are marked with a circle [34]

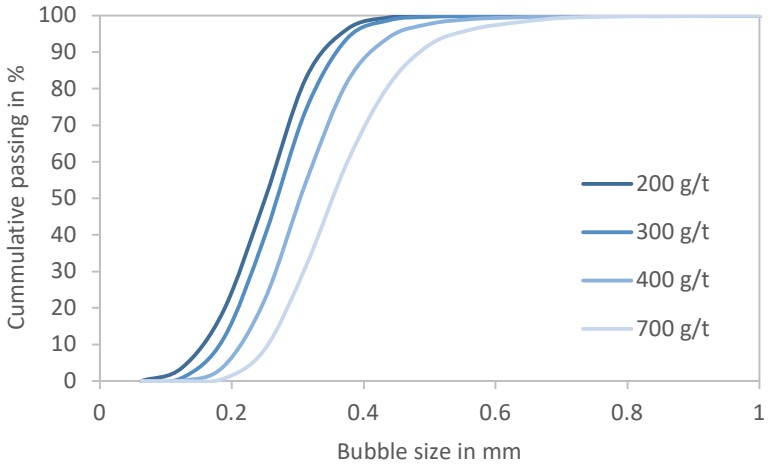

Figure 8. Bubble size distribution as a function of SHMP concentration

3.4. Effect of SHMP on the sedimentation

It is widely known that depressants mostly act as dispersants as well, which has a great capacity of dispersing fine particles; however, it also causes negative pulp effects in the downstream processes, such as in solid-liquid separation, i.e. thickening and filtration. As shown in **Figure 9**, the sedimentation ratio and settling speed decreases with an increase in SHMP concentration. It was observed that the filtration of the tailings after flotation took longer with higher SHMP dosages. Hence, this effect needs to be considered in terms of flotation performance, downstream processes' cost and more importantly, the negative impact on the wastewater when using a high amount of SHMP.

Preprints (www.preprints.org) | NOT PEER-REVIEWED | Posted: 9 April 2021 doi:10.20944/preprints202104.0271.v1

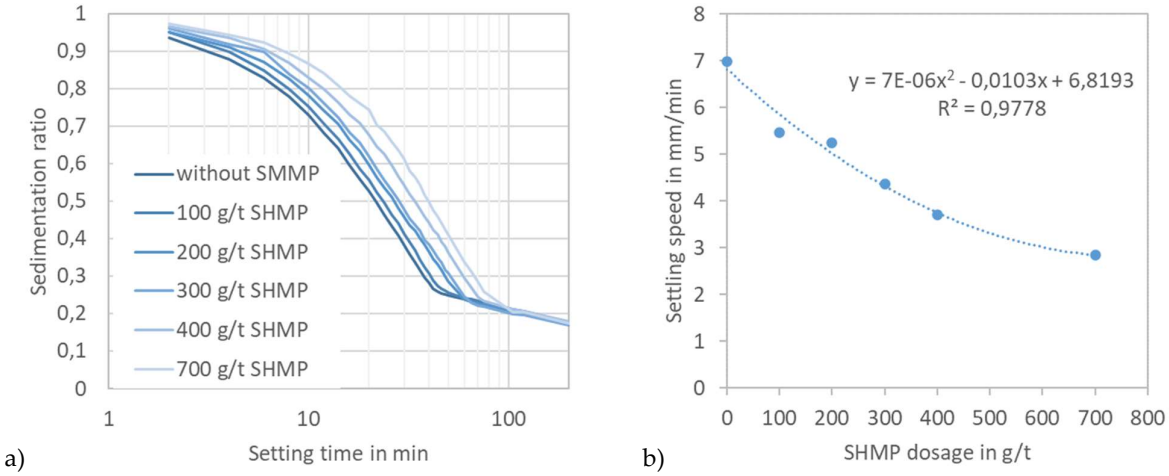

Figure 9. Effect of SHMP on the (**a**) sedimentation ratio and (**b**) settling speed after 2 min in bulk sedimentation

The initial settling velocity is decreased by approximately a factor of two comparing the pulp without SHMP and the pulp containing 700 g/t SHMP. By simple approximation using Stokes' settling velocity relating the velocity to the particle (agglomerated) size squared, that would estimate the agglomerate size to be reduced by a factor of 0.7 due to the dispersing action of SHMP.

3.5. Flotation results

3.5.1. Water pull vs mass pull and liquid content

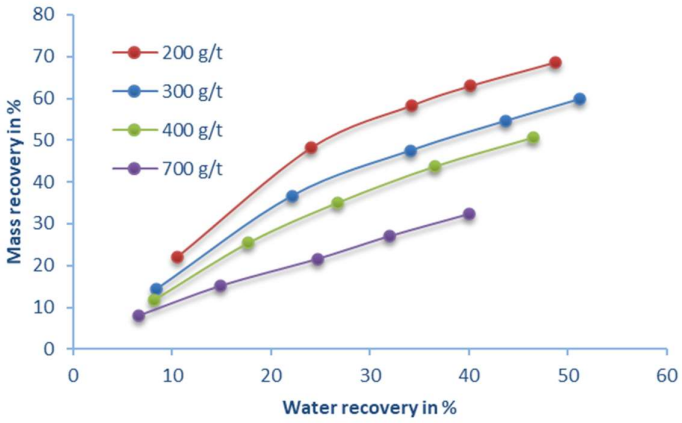

Figure 10. Mass pull vs water pull

As shown with the DFA investigations above SHMP has influenced the froth properties quite significantly, i.e. froth height decreasing with an increase in the concentration of SHMP (**Figure 5**). Another way of looking at the change in froth properties for a given system is plotting mass recovery and water recovery from kinetic flotation tests. **Figure 10** shows the influence of SHMP concentration on these water and mass pulls in the batch flotation tests.

The main finding of the above plot however is that the froth is getting wetter (higher water pull at the same mass pull) with increasing SHMP concentration. Together with the finding that the bubble coalescence in the froth is much stronger as shown with DFA and that the overall particles are better dispersed, this can only mean that the lower mass recovered by particles attached to the bubble surface (i.e. true flotation) and suspended in the lamella (i.e. entrained particles) at the same water recovery, where water can only be recovered

 doi:10.20944/preprints202104.0271.v1

via the lamellae must be governed by lower fraction of true floating particles. Furthermore, **Figure 10** shows the lower mass pull at the same water pull with increasing the SHMP concentration. SHMP is not sufficient to prevent the Resanol A100 collector interacting with mineral surfaces at a low concentration. This leads to an increase in both the recovery of valuable magnesite and true flotation of calcium-carbonate gangue minerals (dolomite and calcite)

3.5.2. Impact of SHMP on the selectivity between magnesite and other gangue minerals

In order to evaluate the separation efficiency of the valuable magnesite from the gangue minerals (dolomite, calcite, and quartz), the selectivity index (*SI*) was defined as a comprehensive evaluation criterion by considering the magnesite content in the feed and the concentrate, i.e., the magnesite and gangue recoveries. The *SI* is given in Eq. 2 [47,50].

$$SI = \sqrt{\frac{R_{mag} \times (100 - R_g)}{(100 - R_{mag}) \times R_g}} \qquad \text{Eq. 2}$$

where R_g is the recovery of gangue mineral in the concentrate, i.e., dolomite, calcite and quartz and R_{mag} denotes the magnesite recovery.

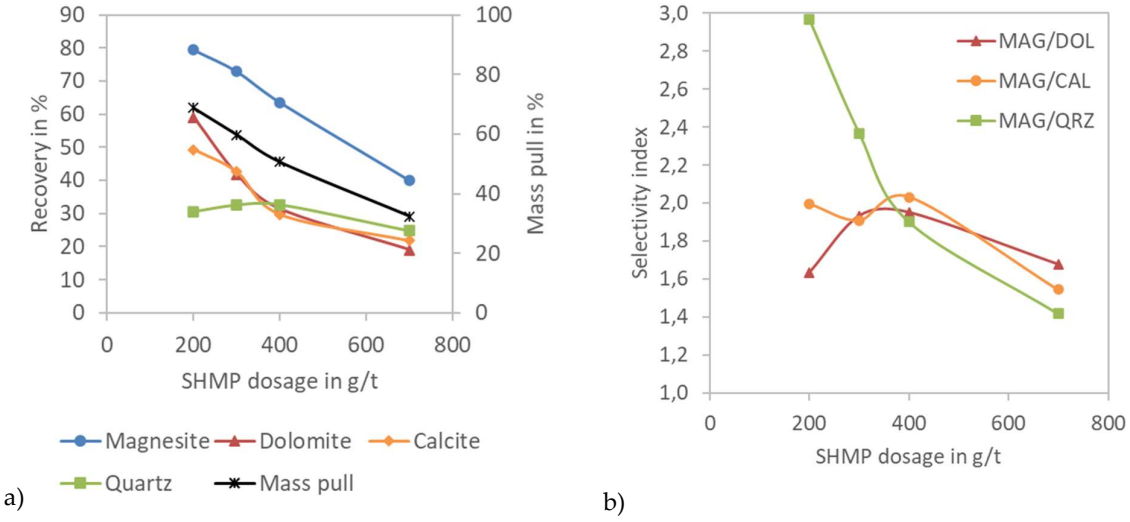

Figure 11. Effect of sodium hexametaphosphate consumption on the recovery (**a**) and (**b**) selectivity between magnesite and gangue minerals

Figure 11a indicates that SHMP not only depressed dolomite and calcite gangue minerals but also strongly influenced the magnesite recovery. SHMP concentration show a linear relationship with the magnesite recovery and mass pull. It demonstrates an effect on the quartz recovery as it ends up in the concentrate mainly by entrainment and as shown before entrainment is affected by SHMP concentration via the dispersion as well as the froth structure. **Figure 11**b also shows the selectivity index between magnesite and other gangue minerals. As shown in **Figure 11**, low SHMP consumption (e.g. below 200 g/t) is not sufficient to prevent the collector absorption on the dolomite and calcite gangue minerals effectively, thus high recoveries of these minerals, resulting in a low selectivity index. At the low SHMP dosage, the dolomite floated well but then floating slower. However, it has a strong effect on the magnesite recovery, as shown in **Figure 11**a, with a linear relationship between magnesite recovery and SHMP dosage.

Figure 12 shows that SHMP has a beneficial impact on the magnesite and dolomite in terms of grade, i.e., magnesite grade increased from 67 % to 77 % and reduced the dolomite content from 29 % to 18 % as the SHMP increased from 200 g/t to 700 g/t. However, there is a trade-off between quality and recovery, when the SHMP increases, magnesite and dolomite recoveries decrease massively, from 80 % to 40 % and 59 % to 20 %, respectively. Surprisingly, the SiO_2 content in the concentrate increased with an increase in SHMP concentration

 doi:10.20944/preprints202104.0271.v1

(**Figure 12**b). As a dispersant, higher SHMP concentration results in better dispersing of the fine particles, making fine quartz particles easier to end up in the froth phase via entrainment. Furthermore, as shown above, an increase in the SHMP concentration leads to a decrease in the settling velocity, thus a lower "drop-back" occurs within the froth zone. In addition, due to the complex interactions between ions and mineral surfaces, the new formation of, i.e., $CaCO_3$, $MgCO_3$, Ca_2SiO_4, or Mg_2SiO_4 on the quartz surface might change its hydrophobicity, thus true flotation of quartz gangue minerals.

It is often emphasized that flotation is a very complex process that is influenced by many factors. Hence, it is a challenge to seek the optimal conditions of individual parameters, due to the interaction between different factors, for example, reactions between the reagents and free ions within the bulk pulp. Hence in this study, we are focusing on the effect of the SHMP, as shown in **Figure 11** that the SHMP dosage is about 300 g/t to 400 g/t gave the best performance. In consequence, this reagent regime is applied for the cleaner flotation study (see section 3.6).

3.5.3. Replacement of SHMP by a novel depressant

1-hydroxyethylene-1,1-diphosphonic acid (HEDP) belongs to the etidronic acid type. It is a rather low toxic and environmentally benign organic phosphate compound that is rather inexpensive and quite common. It is a reagent widely used in water treatment. Yang, Wang, Cao, Yin, Xue, Zhu, Fu and Yao [14] applied on pure minerals, HEDP showed a very promising depressant with very selective depression dolomite. X-ray photoelectron spectroscopy (XPS) and infrared spectrum (IR) analyses indicated that HEDP strongly adsorbed onto the dolomite in advance occupies a large number of calcium sites whereas it had only slightly depressed magnesite. Also, the addition of HEDP prior to sodium oleate (NaOl) had no significant impact on the adsorption of NaOl onto magnesite, while it prevented adsorption of this collector onto dolomite surface [14].

Figure 12a and **Figure 12**b indicate that using only 350 g/t of HEDP can achieve a similar grade (76.3 %) as 700 g/t of SHMP (76.9 %), while it has little effect on the magnesite recovery. The magnesite recovery is about 57 % compared to 40 % when using 700 g/t SHMP. Most importantly, hydrophilic quartz mineral ending up in the concentrate is lower than in the case of using SHMP (**Figure 12**b). HEDP effectively depresses dolomite, resulting in low dolomite grade of 18 % as similar as the case of using 700 g/t SHMP (**Figure 12**c) and showing very good selectivity between magnesite and dolomite (**Figure 12**d).

Preprints (www.preprints.org) | NOT PEER-REVIEWED | Posted: 9 April 2021 doi:10.20944/preprints202104.0271.v1

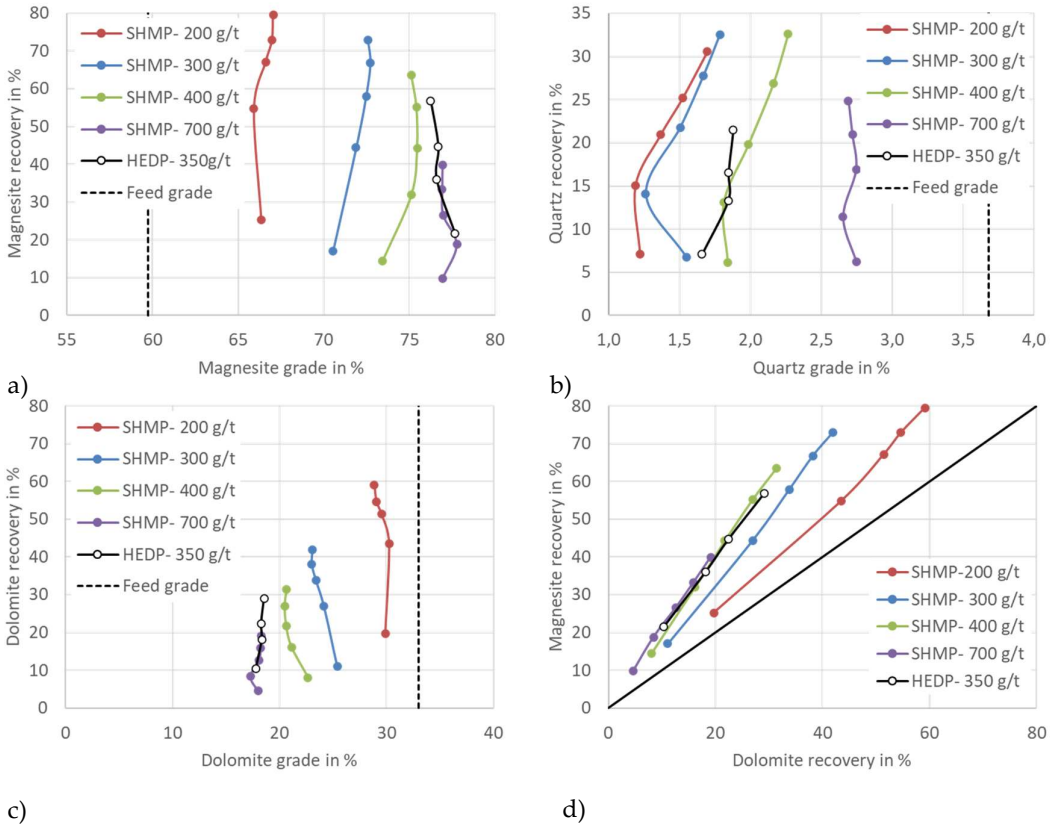

Figure 12. Effect of SHMP and HEDP as the depressants on the grade-recovery a) magnesite, b) quartz, c) dolomite and d) selectivity curves (Fuerstenau upgrading curve) of magnesite against dolomite

3.5.4. Estimation of the degree of entrainment

It is well documented that the entrainment is strongly dependent on the water pull, which is the carrying medium to transfer the entrained particles into the concentrate. For the fine particles, recovery by entrainment is showing a linear relationship with water recovery. **Figure 10** shows both water and mass pull rate increase with the decreasing of the SHMP concentration. The lower water pull results in reducing the degree of entrainment with an increase in SHMP concentration. The entrainment factor *EF* is defined as the ratio of the free gangue particles R_g to water recovery R_w [51,52]. The automated mineralogy data showed quartz is mostly liberated (**Figure 4**). Hence, for the entrainment calculations all the quartz particles were taken into account. This is based on the assumption that solely reaching the concentrate by entrainment.

It is widely known that pulp density has a marked effect on the recovery by entrainment [53-56]. **Figure 13** shows the solids content of the concentrates decreases with an increase in flotation time and at higher SHMP concentrations, resulting in lower pulp density, particularly for the low SHMP concentration. Hence, *EF* decreases with flotation time (**Figure 14**) due to the increasing setting velocity as a decrease in pulp density. Interestingly, for the first concentrate, the *EF* is increasing with an increase in SHMP concentrations. As mentioned above, SHMP influences the state of dispersion, at higher SHMP concentration thus the settling velocity is reduced and fine quartz particles (smallest size, d_P = 6.2 μm (**Figure 1**)) more quickly end up in the froth phase. In contrast, by the end of the flotation test (i.e., concentrates 4 and 5), the different behavior can be seen, as higher SHMP dosage results in decreasing the *EF*, it may be due to the water pull effect with a more stable froth at lower SHMP concentrations. As mentioned above, increasing the SHMP concentration results in decreasing in the dynamic stability factor and half-life time of the bubbles, thus reducing the entrained quartz particles into the concentrate.

Interestingly, using HEDP, the EF is lower compared to SHMP for all the different concentrations. This is another advantage of applying HEDP as a novel depressant, selectively depressing dolomite while reducing the entrained quartz gangue mineral at the same time.

Preprints (www.preprints.org) | NOT PEER-REVIEWED | Posted: 9 April 2021 doi:10.20944/preprints202104.0271.v1

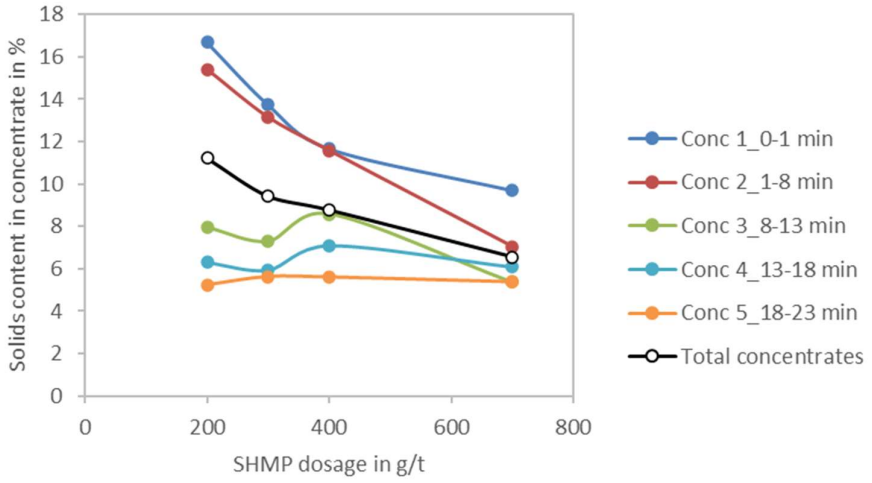

Figure 13. Solid content of concentrates as a function of SHMP concentration and flotation times

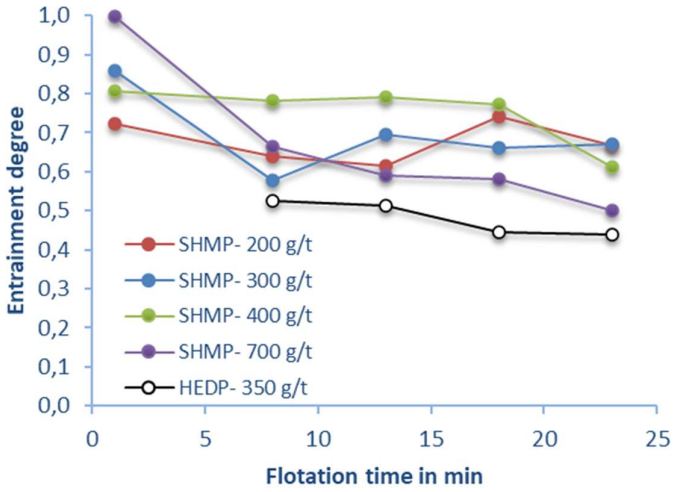

Figure 14. Entrainment factor for quartz minerals as a function of SHMP concentration and flotation times

3.6. Cleaning tests

The 300 g/t concentration of SHMP was considered showing the best performance in terms of selectivity between valuable magnesite and other gangue minerals (dolomite, calcite and quartz) (**Figure 11**). Hence, for this concentration cleaner stages are investigated. With a rougher (two tests) followed by four cleaner steps, a feed ore containing about 59 % magnesite, 33 % dolomite and 4 % quartz was enriched to a concentrate assaying 77.5 % magnesite at a recovery of 45.5 % (**Figure 15**). The dolomite content in the concentrate was about 20 %, where 80 % of dolomite was removed and importantly 98 % of quartz was removed, only 0.3 % of quartz in the final concentrate.

As shown in **Figure 15**, more cleaner stages lead to an increase in the magnesite grade and decrease in the unwanted gangue minerals (i.e., dolomite and quartz). In contrast, this leads to a decrease in the recovery as well. There is a trade-off between the number of cleaner stages to achieve balance in terms of magnesite grade and recovery. The results were performed with the open circuits, however, these trends would be useful to design the flowsheet in order to obtain the final concentrate, which meets the requirement for calcination and sintering in terms of technical and economic considerations.

Preprints (www.preprints.org) | NOT PEER-REVIEWED | Posted: 9 April 2021 doi:10.20944/preprints202104.0271.v1

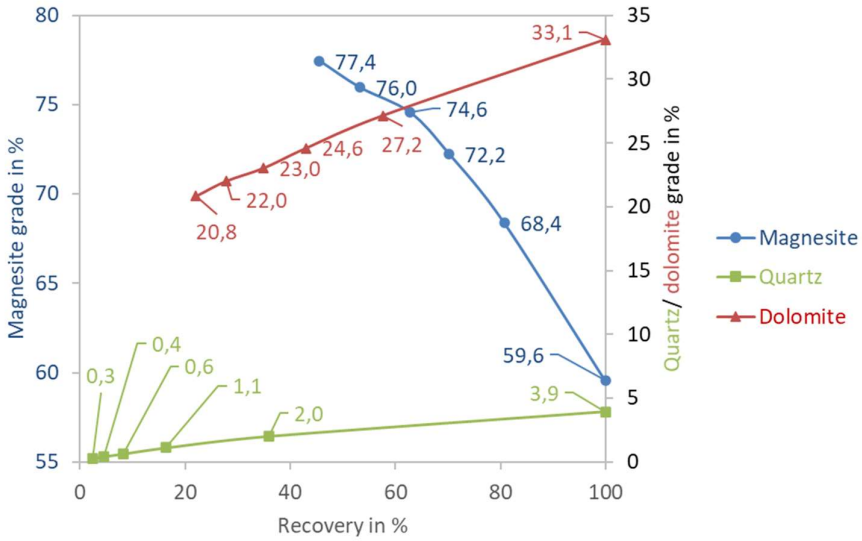

Figure 15. Upgrading the concentrate with cleaning stages

3.7. Interaction within the bulk pulp

Solution thermodynamics of systems containing various suspended semi-soluble salt-type minerals and flotation reagents are rather complex. Magnesite, dolomite and calcite minerals are sparingly soluble and will release their lattice constituents into the solution, resulting in a high Ca^{2+}/ Mg^{2+} ions concentration within the bulk pulp. In addition to the dissolution of minerals and adsorption of dissolved mineral and reagent species at the interface, interactions between these species in the bulk can lead to complicated phenomena such as surface and bulk precipitation as well as re-dissolution of adsorbed species [5].

As can be seen in **Figure 16**, the Ca^{2+}/ Mg^{2+} concentration in the conditioning stage (before reagents added) is higher than their concentration in tap water (*i.e.*, Ca^{2+} ca. 22.5 mg/l, Mg^{2+} ca. 3.7 mg/l). It was also observed that the pH increases during conditioning, which demonstrated that fine minerals were diluted in the solutions. **Figure 16** shows that the ions concentration at the end of flotation reduced significantly, even though the tap water was added to maintain the pulp level. All used reagents (soda Na_2CO_3, sodium silicate Na_2SiO_3, sodium hexametaphosphate $Na_6[(PO_3)_6]$, and Resanol A100 collector) can interact with Ca^{2+} or Mg^{2+} ions or species CO_3^{2-}, SiO_3^{2-} to precipitated calcium/ magnesium silicate, calcite $CaCO_3$, etc. changing the mineral surfaces, and consuming reagents, which is the reason for this significant decrease in ion concentrations (**Figure 16**).

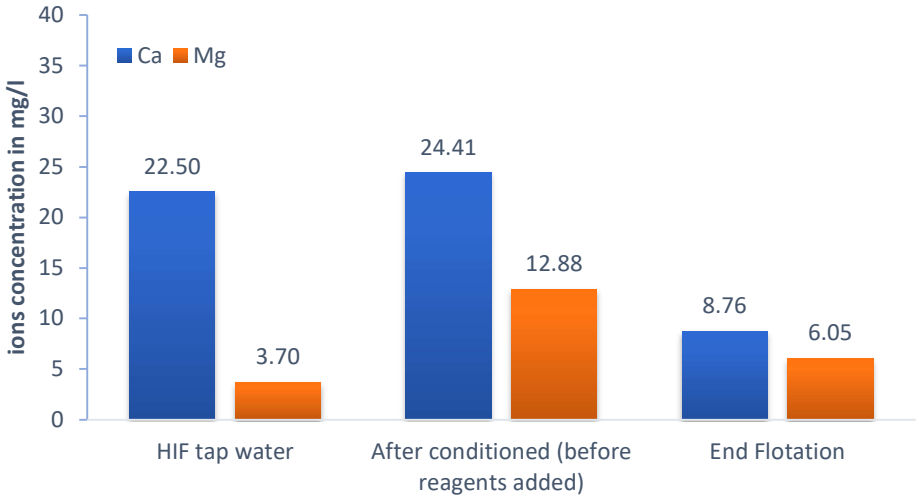

Figure 16. Variation of calcium and magnesium bivalents' concentrations during flotation

 doi:10.20944/preprints202104.0271.v1

4. Conclusion and Recommendations

For the first time a batch flotation study of slime magnesite tailings rich in dolomite is presented. Flotation separation faces many challenges due to ultrafine particles of semi-soluble salt-type minerals and complex interactions between flotation reagents, dissolved ions, species, and mineral surfaces. The depressants, SHMP and HEDP showed to be highly potent in magnesite dolomite-rich flotation not only affecting the flotation performance by means of selectivity but also exposing a significant impact on the pulp and froth properties, and with that influencing downstream processes like dewatering. Through batch flotation testwork on the slime magnesite tailings, sedimentation tests and dynamic froth analysis, the following conclusions were reached:

- A suitable reagent regime has been found to reprocess the desliming fines, currently discarded to the tailing due to mainly lack of flotation technologies.
- With higher SHMP concentration, the magnesite grade was improved while reducing the dolomite content. The reagents consumption is relatively high due to the high specific surface area of fine particles and high Mg^{2+} or Ca^{2+} ion concentration, which could interact with reagents.
- The open circuit with four cleaning stages obtained a concentrate assaying 77.5 % magnesite at a recovery of 45.5 % from slime tailings containing about 59 % magnesite, 33 % dolomite and 4 % quartz. Dolomite content in concentrate is about 20 %, where 80 % of dolomite was removed and importantly 98 % of quartz was removed, only 0.3 % of quartz in the final concentrate.
- As a dispersant, SHMP has a significant influence on the settling speed, thus negatively affecting the downstream processing and wastewater treatment.
- The frothing ability and froth stability, by means of the dynamic stability factor and half-life time of bubbles, decrease when increasing the SHMP concentration, affecting the entrained hydrophilic quartz particles.
- As the SHMP concentration increases, the SiO_2 content increases. The entrainment factor decreases with flotation time due to the significant change in froth properties and pulp density in the case of the batch lab-scale flotation of the rather high-grade ore.
- There is a trade-off when changing the SHMP dosages and the number of cleaner stages to achieve balance in terms of magnesite grade and recovery. These trends would be useful to design the reagents regime and flowsheet in order to obtain the final concentrate, which meets the requirement for calcination and sintering in terms of technical and economic considerations.
- Applying HEDP as a common, and rather cheap reagent shows a promising result that might consider replacing SHMP in the flotation of magnesite rich in dolomite ores.
- The presence of all different flotation reagents (sodium carbonate, sodium silicates, SHMP and collector), dissolved ions and mineral surfaces lead to very complex interactions within the bulk, changing mineral hydrophobicity. Hence, it is noteworthy to consider more fundamental investigations, i.e., the surface charge and the speciation diagram. Furthermore, molecular dynamics simulations can help better understanding the interactions, reagent adsorption and precipitation phenomena.
- With rather low flotation kinetics due to fine and ultrafine particles present, the flotation time was relatively long, at about 23 min. The European FineFuture project (Horizon2020 funding from 2019-2022) is working on innovative technologies, including developing the new reagents, applying the advanced technologies to generate fine bubbles, and a high shear environment, which will improve and speed-up the flotation separation of fine particles. In this context, a pilot Maelgwyn pneumatic/reactor-separator Imhoflot™ G-cells with a throughput up to 5 m^3/h has been constructed and the up-scaling testworks are ongoing and be reported soon.

Author Contributions: Conceptualization, D.H.H. and M.R.; methodology, D.H.H.; D.E., R.M. and M.R.; software, D.H.H. and D.E.; validation, D.H.H., D.E. and R.M.; formal analysis, D.H.H and D.E.; investigation, D.H.H.; resources, D.H.H. and D.E.; data curation, D.E and D.H.H.; writing-original draft preparation, D.H.H.; writing-review and editing, D.H.H., M.R., D.E. and R.M.; visualization, D.H.H.; supervision, M.R. All authors have read and agreed to the published version of the manuscript.

Funding: This paper has received financial support from the European Union's Horizon 2020 research and innovation program under grant agreement N0 821265 - FineFuture.

Acknowledgments: The authors would like to acknowledge Pilar Perez and Antonio Maldonado at Magnesitas Navarras, Spain for their discussions and providing the ore samples in this study. Further thanks to Arsenii Rybalchenko, Luciana Rodrigues de Faria and Juan Sebastian Barajas Narvaez for the sample preparation. Anja Oestreich for conducting the DFA measurements, Kai Bachman for conducting the MLA measurements, Markus Buchmann for his discussions, as well as Klaus Graebe for assisting the sedimentation tests. We would like to thank our colleagues at Maelgwyn Mineral Services for their support, special thanks to Dr. Rainer Imhof for his discussions. To our FineFuture partners and coordinators, many thanks for their discussion and support.

Conflicts of Interest: The authors declare no conflict of interest.

References

1. Wonyen, D.G.; Kromah, V.; Gibson, B.; Nah, S.; Chelgani, S.C. A Review of Flotation Separation of Mg Carbonates (Dolomite and Magnesite). **2018**, *8*, 354.
2. Baudet, G.; Save, M. Phosphoric esters as carbonate collectors in the flotation of sedimentary phosphate ores. **1999**, 163-185.
3. Komar Kawatra, S.; Carlson, J.T. Beneficiation of phosphate ore. *Society for Mining, Metallurgy & Exploration* **2014**.
4. McClellan, G.H.; Van Kauwenbergh, S.J. Mineralogical and chemical variation of francolites with geological time. *Journal of the Geological Society* **1991**, *148*, 809-812, doi:10.1144/gsjgs.148.5.0809.
5. Somasundaran, P.; Wang, D. Chapter 4 Mineral–flotation reagent equilibria. In *Developments in Mineral Processing*, Dianzuo, W., Ed. Elsevier: 2006; Vol. Volume 17, pp. 73-141.
6. Fuerstenau, D.W.; Deason, D.M. Effect of surface transformation processes on the surface chemistry and flotation behavior of dolomite and apatite. In Proceedings of XVII International Mineral Processing Congress; pp. 71-91.
7. Kou, J.; Tao, D.; Xu, G. Fatty acid collectors for phosphate flotation and their adsorption behavior using QCM-D. *International Journal of Mineral Processing* **2010**, *95*, 1-9, doi:http://dx.doi.org/10.1016/j.minpro.2010.03.001.
8. Karlkvist, T. Selectivity in Calcium Mineral Flotation-An analysis of novel and existing approaches. *Doctoral thesis* **2017**.
9. Sis, H.; Chander, S. Reagents used in the flotation of phosphate ores: a critical review. *Minerals Engineering* **2003**, *16*, 577-585, doi:10.1016/s0892-6875(03)00131-6.
10. Smolko-Schvarzmayr, N.; Klingberg, A.; Henriksson, E.; NORDBERG, H. Use of branched alcohols and alkoxylates thereof as secondary collectors 2017.
11. Miller, J.D.; Wang, X.; Li, M. Bench scale flotation of sedimentary phosphate rock with hydroxamic acid collectors. **2002a**, *Zhang, P., El-Shall, H., Somasundaran, P. & Stana R., eds. Proceedings of the Engineering Foundation Conference, Beneficiation of Phosphates III: Fundamentals and Technology*, 93-101.
12. Miller, J.D.; Wang, X.; Li, M. Selective flotation of phosphate minerals with hydroxamate collectors. Google Patents: 2002.
13. Karlkvist, T.; Patra, A.; Rao, K.H.; Bordes, R.; Holmberg, K. Flotation selectivity of novel alkyl dicarboxylate reagents for apatite–calcite separation. *Journal of Colloid and Interface Science* **2015**, *445*, 40-47, doi:https://doi.org/10.1016/j.jcis.2014.11.072.
14. Yang, B.; Wang, D.; Cao, S.; Yin, W.; Xue, J.; Zhu, Z.; Fu, Y.; Yao, J. Selective adsorption of a high-performance depressant onto dolomite causing effective flotation separation of magnesite from dolomite. *Journal of Colloid and Interface Science* **2020**, *578*, 290-303, doi:https://doi.org/10.1016/j.jcis.2020.05.100.
15. Luo, N.; Wei, D.; Shen, Y.; Han, C.; Zhang, C. Elimination of the Adverse Effect of Calcium Ion on the Flotation Separation of Magnesite from Dolomite. **2017**, *7*, 150.
16. Matis, K.A.; Balabanidis, T.H.N.; Gallios, G.P. Processing of magnesium carbonate fines by dissolved-air flotation. **1988**, *29*, 191-203.

17. Matis, K.A.; Gallios, G.P. Anionic flotation of magnesium carbonates by modifiers. *International Journal of Mineral Processing* **1989**, *25*, 261-274, doi:https://doi.org/10.1016/0301-7516(89)90021-5.
18. Yao, J.; Sun, H.; Han, F.; Yin, W.; Hong, J.; Wang, Y.; Won, C.; Du, L. Enhancing selectivity of modifier on magnesite and dolomite surfaces by pH control. *Powder Technology* **2020**, *362*, 698-706, doi:https://doi.org/10.1016/j.powtec.2019.12.040.
19. Gallios, G.P.; Matis, K.A. Floatability of Magnesium Carbonates by Sodium Oleate in the Presence of Modifiers. *Separation Science and Technology* **1989**, *24*, 129-143, doi:10.1080/01496398908049756.
20. Fuerstenau, M.C.; Han, K.N. *Principles of Mineral processing*; SME: 2003.
21. Ozkan, S.G. Beneficiation of magnesite slimes with ultrasonic treatment. *Minerals Engineering* **2002**, *15*, 99-101, doi:https://doi.org/10.1016/S0892-6875(01)00205-9.
22. Luo, X.; Wang, Y.; Wen, S.; Ma, M.; Sun, C.; Yin, W.; Ma, Y. Effect of carbonate minerals on quartz flotation behavior under conditions of reverse anionic flotation of iron ores. *International Journal of Mineral Processing* **2016**, *152*, 1-6, doi:https://doi.org/10.1016/j.minpro.2016.04.008.
23. Li, D.; Yin, W.-z.; Xue, J.-w.; Yao, J.; Fu, Y.-f.; Liu, Q. Solution chemistry of carbonate minerals and its effects on the flotation of hematite with sodium oleate. *International Journal of Minerals, Metallurgy, and Materials* **2017**, *24*, 736-744, doi:10.1007/s12613-017-1457-7.
24. Yao, J.; Yin, W.; Gong, E. Depressing effect of fine hydrophilic particles on magnesite reverse flotation. *International Journal of Mineral Processing* **2016**, *149*, 84-93, doi:https://doi.org/10.1016/j.minpro.2016.02.013.
25. Yin, W.; Sun, H.; Hong, J.; Cao, S.; Yang, B.; Won, C.; Song, M. Effect of Ca selective chelator BAPTA as depressant on flotation separation of magnesite from dolomite. *Minerals Engineering* **2019**, *144*, 106050, doi:https://doi.org/10.1016/j.mineng.2019.106050.
26. Rebolledo, E.; Laskowski, J.S.; Gutierrez, L.; Castro, S. Use of dispersants in flotation of molybdenite in seawater. *Minerals Engineering* **2017**, *100*, 71-74, doi:https://doi.org/10.1016/j.mineng.2016.10.004.
27. Ramirez, A.; Rojas, A.; Gutierrez, L.; Laskowski, J.S. Sodium hexametaphosphate and sodium silicate as dispersants to reduce the negative effect of kaolinite on the flotation of chalcopyrite in seawater. *Minerals Engineering* **2018**, *125*, 10-14, doi:https://doi.org/10.1016/j.mineng.2018.05.008.
28. Li, W.; Li, Y. Improved understanding of chalcopyrite flotation in seawater using sodium hexametaphosphate. *Minerals Engineering* **2019**, *134*, 269-274, doi:https://doi.org/10.1016/j.mineng.2019.02.019.
29. Li, W.; Li, Y.; Xiao, Q.; Wei, Z.; Song, S. The Influencing Mechanisms of Sodium Hexametaphosphate on Chalcopyrite Flotation in the Presence of MgCl2 and CaCl2. **2018**, *8*, 150.
30. Kupka, N.; Rudolph, M. Role of sodium carbonate in scheelite flotation – A multi-faceted reagent. *Minerals Engineering* **2018**, *129*, 120-128, doi:https://doi.org/10.1016/j.mineng.2018.09.005.
31. Hasson, D.; Shemer, H.; Sher, A. State of the Art of Friendly "Green" Scale Control Inhibitors: A Review Article. *Industrial & Engineering Chemistry Research* **2011**, *50*, 7601-7607, doi:10.1021/ie200370v.
32. Huang, Z.; Wang, J.; Sun, W.; Hu, Y.; Cao, J.; Gao, Z. Selective flotation of chalcopyrite from pyrite using diphosphonic acid as collector. *Minerals Engineering* **2019**, *140*, 105890, doi:https://doi.org/10.1016/j.mineng.2019.105890.
33. Wang, J.; Zhou, Z.; Gao, Y.; Sun, W.; Hu, Y.; Gao, Z.J.M. Reverse flotation separation of fluorite from calcite: a novel reagent scheme. **2018**, *8*, 313.
34. Hoang, D.H.; Heitkam, S.; Kupka, N.; Hassanzadeh, A.; Peuker, U.A.; Rudolph, M. Froth properties and entrainment in lab-scale flotation: A case of carbonaceous sedimentary phosphate ore. *Chemical Engineering Research and Design* **2019**, *142*, 100-110, doi:https://doi.org/10.1016/j.cherd.2018.11.036.
35. Farrokhpay, S. The significance of froth stability in mineral flotation--a review. *Advances in colloid and interface science* **2011**, *166*, 1-7, doi:10.1016/j.cis.2011.03.001.
36. Schwarz, S. The relationship between froth recovery and froth structure. University of South Australia, 2004.
37. Pugh, R.J. Foaming, foam films, antifoaming and defoaming. *Advances in colloid and interface science* **1996**, *64*, 67-142, doi:https://doi.org/10.1016/0001-8686(95)00280-4.
38. Bikerman, J.J. *Foams*; Springer-Verlag: New York, 1973; 10.1007/978-3-642-86734-7.

39. Mackay, I.; Mendez, E.; Molina, I.; Videla, A.R.; Cilliers, J.J.; Brito-Parada, P.R. Dynamic froth stability of copper flotation tailings. *Minerals Engineering* **2018**, *124*, 103-107, doi:https://doi.org/10.1016/j.mineng.2018.05.005.
40. McFadzean, B.; Achaye, I.; Chidzanira, T.; Harris, M. The effect of particle size on froth stabilities of different ores. In Proceedings of XXVIII International Mineral Processing Congress Proceedings, Quebec, Canada.
41. McFadzean, B.; Marozva, T.; Wiese, J. Flotation frother mixtures: Decoupling the sub-processes of froth stability, froth recovery and entrainment. *Minerals Engineering* **2016**, *85*, 72-79, doi:https://doi.org/10.1016/j.mineng.2015.10.014.
42. Heinig, T.; Bachmann, K.; Tolosana-Delgado, R.; Van Den Boogaart, G.; Gutzmer, J. Monitoring gravitational and particle shape settling effects on MLA sampling preparation. In Proceedings of Proceedings of IAMG; pp. 200-206.
43. Fandrich, R.; Gu, Y.; Burrows, D.; Moeller, K. Modern SEM-based mineral liberation analysis. *International Journal of Mineral Processing* **2007**, *84*, 310-320.
44. Hoang, D.H.; Kupka, N.; Peuker, U.A.; Rudolph, M. Flotation study of fine grained carbonaceous sedimentary apatite ore – Challenges in process mineralogy and impact of hydrodynamics. *Minerals Engineering* **2018**, *121*, 196-204, doi:https://doi.org/10.1016/j.mineng.2018.03.021.
45. Leißner, T.; Hoang, D.H.; Rudolph, M.; Heinig, T.; Bachmann, K.; Gutzmer, J.; Schubert, H.; Peuker, U.A. A mineral liberation study of grain boundary fracture based on measurements of the surface exposure after milling. *International Journal of Mineral Processing* **2016**, *156*, 3-13, doi:https://doi.org/10.1016/j.minpro.2016.08.014.
46. Doebelin, N.; Kleeberg, R. Profex: a graphical user interface for the Rietveld refinement program BGMN. *Journal of Applied Crystallography* **2015**, *48*, 1573-1580, doi:doi:10.1107/S1600576715014685.
47. Hoang, D.H.; Hassanzadeh, A.; Peuker, U.A.; Rudolph, M. Impact of flotation hydrodynamics on the optimization of fine-grained carbonaceous sedimentary apatite ore beneficiation. *Powder Technology* **2019**, *345*, 223-233, doi:https://doi.org/10.1016/j.powtec.2019.01.014.
48. Boos, J.; Drenckhan, W.; Stubenrauch, C. Protocol for Studying Aqueous Foams Stabilized by Surfactant Mixtures. *Journal of Surfactants and Detergents* **2013**, *16*, 1-12, doi:10.1007/s11743-012-1416-2.
49. Wang, Y.; Neethling, S.J. The relationship between the surface and internal structure of dry foam. *Colloids and Surfaces A: Physicochemical and Engineering Aspects* **2009**, *339*, 73-81, doi:https://doi.org/10.1016/j.colsurfa.2009.01.021.
50. Gaudin, A.M. *Principles of Mineral Dressing*; McGraw-Hill: New York, 1939.
51. Johnson, N.W. *The flotation behaviour of some chalcopyrite ores*; University of Queensland Press: St. Lucia, Queensland, 1972.
52. Yianatos, J.; Contreras, F. Particle entrainment model for industrial flotation cells. *Powder Technology* **2010**, *197*, 260-267, doi:https://doi.org/10.1016/j.powtec.2009.10.001.
53. Wang, L.; Peng, Y.; Runge, K. Entrainment in froth flotation: The degree of entrainment and its contributing factors. *Powder Technology* **2016**, *288*, 202-211, doi:10.1016/j.powtec.2015.10.049.
54. Zheng, X.; Johnson, N.W.; Franzidis, J.P. Modelling of entrainment in industrial flotation cells: Water recovery and degree of entrainment. *Minerals Engineering* **2006**, *19*, 1191-1203, doi:10.1016/j.mineng.2005.11.005.
55. Yianatos, J.; Contreras, F.; Díaz, F.; Villanueva, A. Direct measurement of entrainment in large flotation cells. *Powder Technology* **2009**, *189*, 42-47, doi:10.1016/j.powtec.2008.05.013.
56. Johnson, N. A review of the entrainment mechanism and its modelling in industrial flotation processes. **2005**.